

Photocatalytic Degradation of Metronidazole Using Zinc Oxide Nanoparticles Supported on Acha Waste

Olushola Sunday Ayanda^{1*}, Blessing Oluwatobi Adeleye¹, Omolola Helen Aremu¹, Folasade Busayo Ojobola², Olayide Samuel Lawal¹, Olusola Solomon Amodu³, Oyedele Oyebamiji Oketayo⁴, Michael John Klink⁵, and Simphiwe Maurice Nelana⁵

¹Nanoscience Research Unit, Department of Industrial Chemistry, Federal University Oye Ekiti, P.M.B. 373, Oye Ekiti, Ekiti State, Nigeria

²Department of Science Education, Federal University Oye Ekiti, P.M.B. 373, Oye Ekiti, Nigeria

³Department of Chemical Engineering, Lagos State Polytechnic, P.M.B. 21606, Ikorodu, Lagos, Nigeria

⁴Department of Physics, Federal University Oye Ekiti, P.M.B. 373, Oye Ekiti, Nigeria

⁵Department of Chemistry, Vaal University of Technology, Vanderbijlpark 1900, South Africa

* **Corresponding author:**

email: osayanda@gmail.com

Received: June 20, 2022

Accepted: September 15, 2022

DOI: 10.22146/ijc.75585

Abstract: The presence of emerging pollutants like pharmaceutical compounds in the environment is currently an issue of concern. Pharmaceutical compounds often escape conventional treatment systems and are persistent in the receiving environment; thus, the advanced oxidation processes could complement existing treatment methods to completely remove pharmaceuticals from contaminated water bodies. This work investigated the removal of metronidazole by ultra-violet light catalyzed by zinc oxide nanoparticles supported on acha waste. The synthesized zinc oxide nanoparticles, acha waste, and zinc oxide nanoparticles/acha waste composite were characterized by electron microscopy (SEM and TEM), Fourier transforms infrared spectrometry (FTIR) and X-ray diffractometry (XRD). Experimental results revealed that the UV light combined with zinc oxide nanoparticles and/or acha waste was more effective for metronidazole removal in combination than UV alone. The degradation of the metronidazole by UV light only, UV/nano-ZnO, and UV/nano-ZnO/acha waste systems follow the pseudo-first-order kinetic model. The addition of a catalyst to the UV reactor enhanced the degradation of metronidazole (5 mg/L) from 41.0 up to 86.1%. The outcome of this research showed that UV light in the presence of nanometal oxides and composites is an efficient technique for the removal of pharmaceuticals from an aqueous solution.

Keywords: metronidazole; zinc oxide nanoparticles; acha waste; UV light; photocatalysis

■ INTRODUCTION

Pharmaceutical industries are major sectors that contribute to an increase in the presence of toxic pollutants and hazardous chemicals in the environment [1-2]. Due to the high production of pharmaceuticals resulting from its growing demand, there is an increase in the generation of pharmaceutical wastewater (PWW). PWW, when not properly regulated and treated before disposal into the environment, can cause adverse effects

on plants, animals, soil, groundwater resources, aquatic organisms, and humans present in the environment. The degree of toxicity depends on the type of pharmaceutical product involved. PWW contains a high amount of various organic pollutants, COD, BOD, and suspended solids with varying colors [3]. PWW can be formed through i) improper treatment of waste obtained from the production process of the pharmaceuticals, ii) hospital effluents because of the numerous pharmaceuticals used in the treatment of patients, iii)

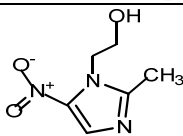
human and animal excretions when treated with pharmaceutical products, and iv) unused drugs disposed into the environment. Metronidazole (MNZ), a common synthetic pharmaceutical antibiotic, is used in destroying or inhibiting the growth of bacteria caused by microorganisms such as *Giardia lamblia*, *Trichomonas vaginalis*, *Entamoeba histolytica*, and *Clostridium difficile* [4]. MNZ is used majorly in treating vagina infections, gastrointestinal infections, pelvic inflammatory disease, rosacea, and pneumonia [5]. The use of MNZ can cause certain side effects such as diarrhea, nausea, abdominal pain [5], vomiting, constipation, loss of appetite, and rashes [6]. Most times, these side effects occur when MNZ is taken alongside alcohol or food whose constituents can agitate the effects [7]. MNZ is usually administered orally through the mouth, intravenously by the use of injection into the vein and is also available for use in the form of cream [8]. Due to its non-biodegradability, MNZ can bioaccumulate in the environment, survive in the aquatic environment for longer periods [9] and can therefore result in the presence of antibiotic resistant bacteria in the environment [10]. The chemical structure and some important properties of MNZ are presented in Table 1.

Various conventional methods, which include the physical (sedimentation, coagulation, flocculation, and filtration), biological (use of microorganisms in degrading pollutants) and chemical (disinfection, neutralization, adsorption, ion exchange) methods, have been used in the removal of MNZ from wastewater. However, they are not efficient enough since PWW

contains a high concentration of toxic, organic and hazardous pollutants. A more convenient, effective and efficient method for PWW treatment is the advanced oxidation processes (AOPs). AOP, a promising technique sometimes referred to as the tertiary treatment of wastewater, involves reactions of pollutants with hydroxyl radicals to remove organic and inorganic pollutants in wastewater [11].

The treatment of wastewater via photocatalysis allows the creation of electron-hole pairs by the catalyst, which leads to the generation of free radicals. The hydroxyl radical generated helps in converting toxicants pollutants present in the wastewater to non-dangerous and less harmful substances [12]; the organic pollutants present are converted into CO₂ and H₂O. Farzadkia et al. [13] studied the degradation of MNZ in an aqueous solution by nano-ZnO/UV photocatalytic process. In their study, the effects of some operational parameters such as pH, time, nano-dosage, and power of radiation on the degradation efficiency of MNZ wastewater using zinc oxide nanoparticles as a photocatalyst were investigated. Results showed that the removal of MNZ and chemical oxygen demand (COD) has a direct correlation with the power of the UV-A lamp and irradiation time. Also, in the experiment carried out, 96.55% degradation was achieved. Fang et al. [14] researched the effective removal of MNZ from water by nanoscale zero-valent iron (nZVI) particles. In their study, it was reported that the removal of MNZ by nZVI followed pseudo-first order kinetics, and the removal is

Table 1. Chemical structure and properties of metronidazole

Chemical structure	
IUPAC name	(2-methyl-5-nitroimidazole-1-ethanol)
Molar mass	171.156 g/mol
Melting point	159 to 163 °C
Color	yellow, white
Solubility	Soluble in water (10 mg/mL at 20 °C); ethanol (5 mg/mL); methanol, chloroform, and ether (< 0.5 mg/mL); DMSO (34 mg/mL at 25 °C); and dilute acids
Synonym	Flagyl

influenced by several factors such as nZVI dosage, initial MNZ concentration and initial solution pH. The authors reported that the MNZ solution at 80 mg/L was removed rapidly by nZVI in 5 min, at an initial solution of pH 5.60 and catalyst dosage of 0.1 g/L. Farzadkia et al. [15] investigated the degradation of aqueous MNZ with illuminated TiO₂-NP_s at different catalyst dosages, time, pH, initial MNZ concentration, and light intensity. In their study, it was observed that maximum removal of MNZ occurs at near neutral pH, the rate of removal decreases by dosage increase, and increase in initial MNZ concentration. Moreover, the authors reported that the reaction rate constant (k_{obs}) decreased from 0.0513 to 0.0072 min⁻¹, and the value of electrical energy per order (E_{EO}) increased from 93.57 to 666.67 (kWh/m³) with an increasing initial MNZ concentration from 40 to 120 mg/L.

Acha, commonly referred to as “fonio” is a species of the grass family and one of the ancient African crops [16]. It has other common names such as “hungry rice” (English), “fonyo” (Fulani), and “fini” (Bambara). Acha is mainly of two species, white fonio (*Digitaria exilis*) and black fonio (*Digitaria iburua*). Of the two species, the white fonio is commonly used and is grown particularly on the upland Plateau of Central Nigeria as well as its neighboring regions, with the black specie limited to the Jos-Bauchi Plateau of Nigeria [17]. The acha grains serve as a great source of food as they are used as rice, made into porridge and couscous, for bread and beer making process. Moreover, acha has great usefulness as a source of starch after it has undergone various processes, with acha chaff as waste resulting from acha processing. The use of acha waste in environmental remediation will provide a better means of utilizing the waste than disposing it into the environment, thereby reducing pollution, which can cause damage to the ecosystem. It also reduces cost when compared to the high cost of other chemicals used in wastewater treatment, and it helps in improving economic stability by use of other simpler methods in effecting a change in the environment.

The objective of this study is to investigate the removal of MNZ from an aqueous solution using ultra-violet (UV) light in the presence of catalysts (zinc oxide nanoparticles, acha waste (agricultural waste), and zinc

oxide nanoparticles/acha waste composite). Operating parameters such as the effect of time, catalyst dosage, initial MNZ concentration and solution pH were considered in the course of the investigation.

■ EXPERIMENTAL SECTION

Materials

Winnowed acha grains were collected from a local market in Jos, Plateau State. MNZ and sodium hydroxide pellets (98% pure) were purchased from Sigma Aldrich, whereas zinc chloride (97% pure) was purchased from Loba Chemie Pvt. Ltd., India. The stock solution of MNZ was prepared by dissolving a suitable amount of MNZ in 1 L of deionized water in a standard volumetric flask. Serial dilution of the stock was used to prepare the working solutions.

Instrumentation

The surface morphological study of zinc oxide nanoparticles and zinc oxide nanoparticles/acha waste composite was carried out using TESCAN MIRA3 and JSM-7600F SEM, respectively. The sample was observed at 7000–9000× magnification with an accelerating voltage of 15 Kv [19]. TEM analysis of the zinc oxide nanoparticles was by Tecnai G2 20, and the FTIR spectra of the nanoparticles and composite were obtained using Universal Attenuated Total Reflectance (UATR) Infrared spectrometer Perkin Elmer Spectrum 2 recorded over 400–4000 cm⁻¹ range. To capture the diffraction patterns of the samples, an X-ray diffractometer (D8 Advance, BRUCER AXS, Karlsruhe, Germany) operating at Bragg angle (2θ) in the range of (3–40 °C) with scan step (0.035°), step time (0.5 s), and generator settings (40 Kv, 40 mA) was used [20].

Procedure

Extraction of acha starch and separation of chaff

The winnowed acha grain was stepped into water for 6 h, after which the solution was discarded. The swollen grain was washed with water and blended using a domestic milling machine. The slurry (a mixture of starch and chaff) obtained was suspended in water (5 L) and was adjusted to pH 8 using NaOH (0.1 M). The starch slurry was sieved until the starch had been

separated from the chaff. Thereafter, the chaff (acha waste) was air-dried for 24 h and further dried in the oven for 48 h at 100 °C.

Preparation of nano zinc oxide/acha waste composite

The method by Ayanda et al. [18] was used in the synthesis of zinc oxide nanoparticles (Fig. 1) and to prepare the composite, 0.5 g of zinc oxide nanoparticles was mixed thoroughly with 5 g of the acha chaff before the material was air and oven dried at 100 °C.

Photolysis

During this experiment, photolytic treatment (ultra-violet light only) of aqueous MNZ was observed under the effect of time, pH and concentration. For the effect of time on the degradation of MNZ, aqueous MNZ (20 mL) was placed in a beaker, and a UV lamp with a wavelength of 254 nm was placed above the reactor containing the solution, 14 cm is the distance between the UV lamp and the aqueous MNZ. The time intervals investigated were 10, 20, 30, 40, and 60 min. To investigate the effect of pH, varying pH range (2–10) was used. MNZ concentrations of 5, 2.5, 1.25, 0.625, and 0.3125 mg/L at pH 2 and time of 60 min were utilized during the investigation of the effect of initial MNZ concentration.

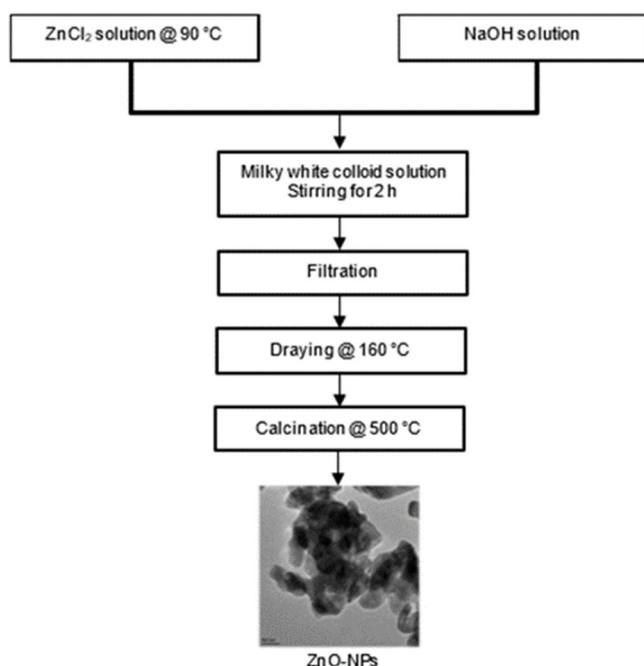


Fig 1. Flowchart for the synthesis of zinc oxide nanoparticles

Photocatalysis

Photocatalysis was also considered at a wavelength of 254 nm; moreover, the effect of time, catalyst dosage, pH, and concentration were examined. Zinc oxide nanoparticles and zinc oxide nanoparticles/acha waste composite were used as catalysts. For the effect of time, 20 mL of aqueous MNZ containing catalyst (0.02 g) was placed in a beaker, and the UV lamp was placed above the reactor containing the solution. The time intervals investigated were between 10–60 min. The effect of the amount of catalyst dosage on the degradation of MNZ was achieved by placing 20 mL of aqueous MNZ in a beaker containing 0.02–0.1 g of the catalyst for 60 min. To investigate the effect of pH, the experiment was conducted by varying the pH from 2 to 10. Lastly, the effect of initial MNZ concentration on the photocatalytic degradation of MNZ was achieved using MNZ at concentrations of 5, 2.5, 1.25, 0.625, and 0.3125 mg/L, the pH of the solution was kept at 2 and a contact time of 60 min.

After the completion of each experiment, samples were taken (filtered in the case of photocatalysis) and analyzed using a BIOBASE BK-UV1900BC spectrophotometer at a wavelength of 320 nm [21]. The percentage degradation was calculated using Eq. (1).

$$\% \text{ Degradation} = \frac{\text{MNZ}_0 - \text{MNZ}_f}{\text{MNZ}_0} \times 100 \quad (1)$$

where MNZ_0 and MNZ_f are the initial and final concentrations of MNZ (mg/L), respectively.

RESULTS AND DISCUSSION

The Results of FTIR and XRD

The FTIR bands observed in the spectra of zinc oxide nanoparticles and zinc oxide nanoparticles/acha waste composite are presented in Table 2. The peaks observed at 469.11 and 460.84 cm^{-1} correspond to the Zn-O group [22]. A strong and broad band observed at 3448.94 cm^{-1} corresponds to the O-H stretching mode of hydroxyl groups [23], and this indicates the contribution of water molecules. The FTIR band at 2927 cm^{-1} could be assigned to aliphatic νCH_2 symmetric frequency and may be due to the presence of ethanol in the acha waste. The band at 1644.13 cm^{-1} may be due to

Table 2. Absorption bands of zinc oxide nanoparticles, acha waste and zinc oxide nanoparticles/acha waste composite

S/N	Zinc oxide nanoparticles (cm ⁻¹)	Acha waste	Zinc oxide nanoparticles/acha waste composite (cm ⁻¹)
1	469.11	3448.94	3448.94
2	460.84	2927.70	2927.70
3		1644.13	1644.13
4		1155.57	1155.57
5		1080.35	1080.35
6		1019.76	1019.76
7		713.86	713.86
8			469.11

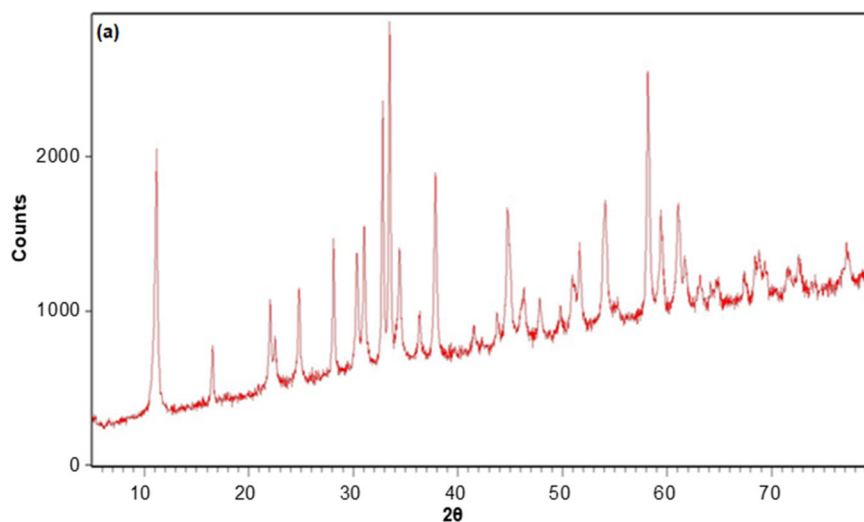
the double bonds ($-C=C-$), carbonyl bonds ($-C=O$) groups stretching vibration and may be related to the aromatic ring deformation associated with polyphenol compounds. The FTIR bands at 1155.57, 1080.35, and 1019.76 cm^{-1} may be linked to sugar moiety attached to polyphenols; moreover, they may be related to the aromatic $-OH$ group vibration and symmetry stretching of $-C-C-$. The band at 713.86 cm^{-1} may be related to aromatic ring vibration [24]. The presence of all the FTIR bands associated with zinc oxide nanoparticles and acha waste in the zinc oxide nanoparticles/acha waste composite indicated that the two precursors interacted.

The XRD patterns provided having 2θ values with strong diffraction peaks appear at 10.9°, 15.2°, 24.3°, 37.8°, and 57.6° (Fig. 2(a)) and 10.8°, 27.9°, 22.2°, 33°, 37.8°, and 57.6° (Fig. 2(b)). The XRD pattern indicated that the zinc oxide nanoparticles are crystalline, having a wurtzite

crystalline structure with a hexagonal phase, and no characteristic diffraction peaks other than zinc oxide nanoparticles were observed [25]. The zinc oxide nanoparticles/acha waste composite tends to be amorphous after the addition of zinc oxide nanoparticles and acha waste, as depicted in Fig. 2(b).

The SEM and TEM Results

The SEM and TEM of zinc oxide nanoparticles in Fig. 3(a) and 3(b) showed that the zinc oxide nanoparticles are agglomerated, and there's no complete separation between them. The TEM micrograph also confirmed the presence of multiple hexagonal structures in mass. This result may be due to weak physical force holding the particles together [26]. Fig. 3(c) shows that the composite material has an irregular, non-smooth surface with more large size pores [20].



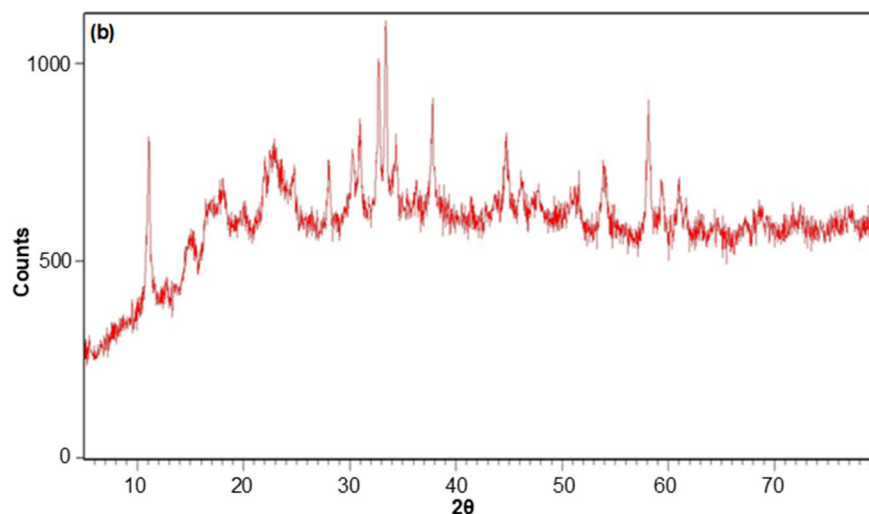


Fig 2. XRD patterns of zinc oxide nanoparticles (a) and zinc oxide nanoparticles/acha waste composite (b)

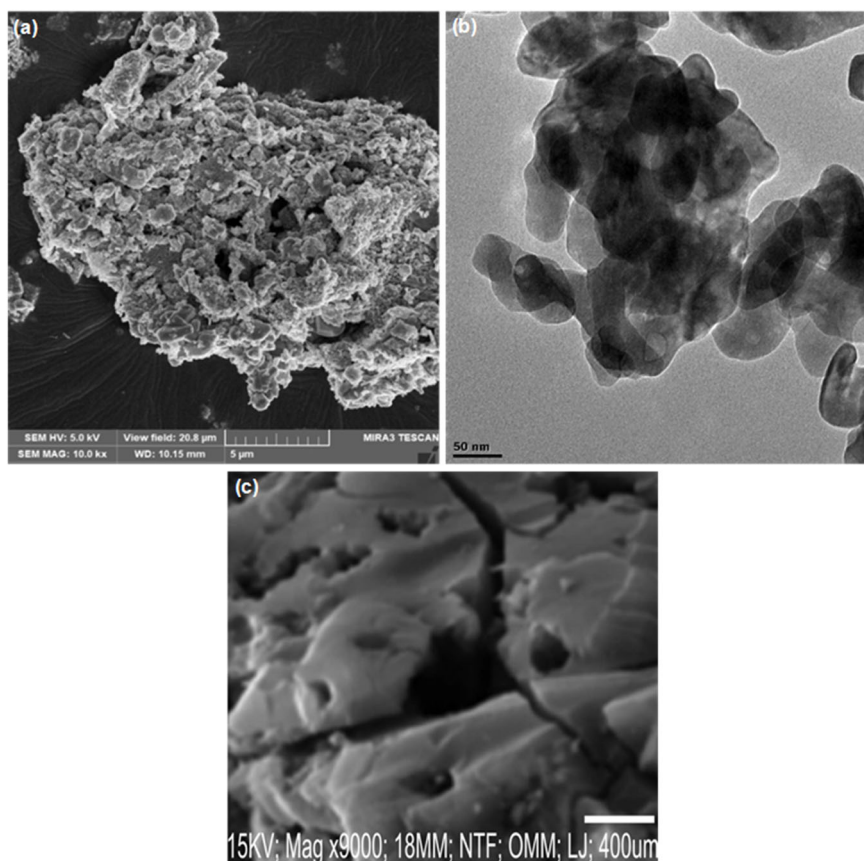


Fig 3. SEM (a) and TEM (b) micrographs of zinc oxide nanoparticles, and SEM of zinc oxide nanoparticles/acha waste composite (c)

Degradation of Aqueous Metronidazole

Effect of time of exposure

Fig. 4 shows the effect of time on the degradation of the MNZ solution. The figure indicated that the

percentage degradation increases and improves with time. For the photolysis (UV only), the percentage degradation increases from 30.2 ± 0.2 to $64.0 \pm 0.2\%$. The UV/nano-ZnO and UV/nano-ZnO/acha waste systems

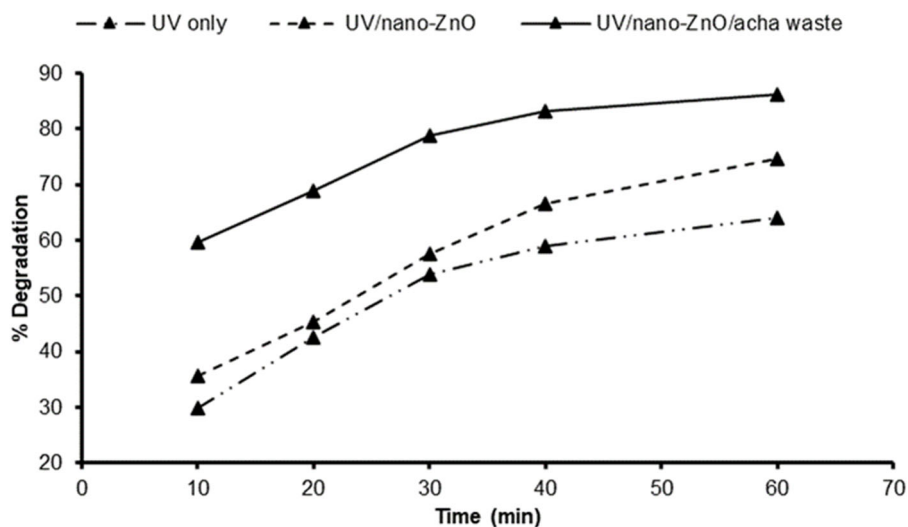


Fig 4. Effect of contact time on the degradation of metronidazole using UV, UV/nano-ZnO and UV/nano-ZnO/acha waste systems

resulted in 35.7 ± 0.3 to $74.7 \pm 0.3\%$ and 59.7 ± 0.2 to $86.1 \pm 0.2\%$, respectively. The highest degradation efficiency with photocatalysis (UV/nano-ZnO and UV/nano-ZnO/acha waste), when compared to UV light only, might be due to the synergistic effect between the UV light, zinc oxide nanoparticles and acha waste. The result obtained is similar to previous studies on the degradation of amoxicillin, ampicillin and cloxacillin antibiotics by Moradmand Jalali and Dezhampannah [27].

Effect of initial MNZ concentration

The effect of initial MNZ concentration on the

photolytic and photocatalytic degradation of MNZ solution is presented in Fig. 5. The figure showed that the percentage degradation of MNZ decreases as the initial concentration of MNZ increases from 0.3125 to 5.0 mg/L. For UV only, $3.47 \pm 0.2\%$ of MNZ was degraded at 5.0 mg/L MNZ initial concentration, whereas an MNZ solution of 0.3125 mg/L resulted in $74.1 \pm 0.2\%$ degradation. The UV/nano-ZnO and UV/nano-ZnO/acha waste systems resulted in $54.7 \pm 0.1 - 81.4 \pm 0.1\%$ and 73.9 ± 0.2 to $98.9 \pm 0.2\%$, respectively, when the concentration of MNZ was varied from 5.0 to 0.3125 mg/L.

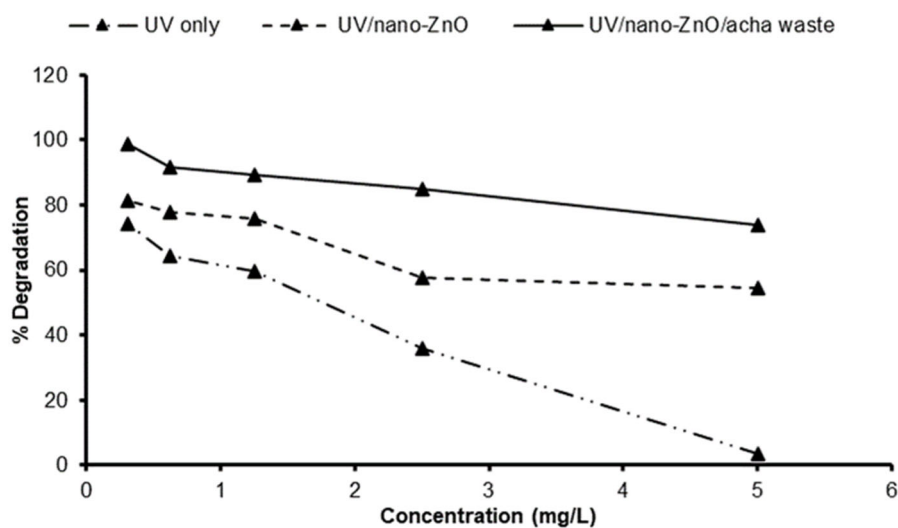


Fig 5. Effect of initial concentration on the degradation of metronidazole using UV, UV/nano-ZnO and UV/nano-ZnO/acha waste systems

The results obtained are similar to the work reported by Farzadkia et al. [15]. The authors reported that the photocatalytic degradation of MNZ with illuminated TiO₂ nanoparticles decreased with increasing initial MNZ concentration. The reason for this observation was presumed to be i) the surface of the catalyst might be occupied by MNZ as the initial MNZ concentration increases, ii) more degradation intermediates can be accumulated on the catalyst surface, causing a negative effect in the utilization of hydroxyl radicals or positive holes in the valence band of the catalyst surface, and iii) inner filtration effect which causes a decrease of photon reaching the catalyst surface.

Effect of solution pH

Fig. 6 shows the effect of pH on the degradation of the MNZ solution. The percentage degradation of MNZ by UV light increases from $1.33 \pm 0.1\%$ in the basic medium to $76.27 \pm 0.1\%$ in the acidic medium. Therefore, the degradation of the MNZ solution could be said to be favored in the acidic medium over the basic medium. The point of zero charges (pH_{pzc}) of zinc oxide nanoparticles was estimated at about 8.3–9.0 [28–29]. This implies that at pH values below the pH_{pzc} , the surface of zinc oxide nanoparticles has a net positive charge, whereas, at pH greater than the pH_{pzc} , the surface of zinc oxide nanoparticles has a net negative charge. Thus, at low pH value, the surfaces of zinc oxide nanoparticles were highly

protonated and became positively charged so that the MNZ anion was electrostatically attracted towards the catalyst surface.

Similarly, the same trends were observed for the UV/nano-ZnO and UV/nano-ZnO/acha waste systems. The percent degradation decreased from 70.9 ± 0.2 to $10.9 \pm 0.2\%$ as the pH of the solution was increased from 2 to 10 during UV/nano-ZnO degradation of 5 mg/L MNZ solution. The UV/nano-ZnO/acha waste MNZ treatment system resulted to a reduction in the percent degradation from 76.9 ± 0.2 to $18.4 \pm 0.2\%$ as the pH of the solution was increased from pH 2 to 10. Farzadkia et al. [15] obtained the highest degradation efficiency of MNZ at neutral pH (pH 7) with the lowest degradation at pH 11; moreover, the removal efficiency of MNZ by Asgharzadeh et al. [30] increased as the pH increased from 3 to 7; nevertheless, the efficiency decreased with further increase in pH value from 9 to 11. Thus, the trend observed in this study could be explained by the variation of charges on MNZ ($pK_a = 2.55$) as well as on the surface of the catalyst at different solution pH.

Effect of catalyst dosages

Fig. 7 shows the effect of catalyst dosages (0.02–0.1 g) on the photocatalytic degradation of MNZ at a pH of 2, observed for 60 min. The degradation efficiency decreased as the nano dosage increased from 0.02–0.1 g. The decrease in the degradation efficiencies of MNZ might

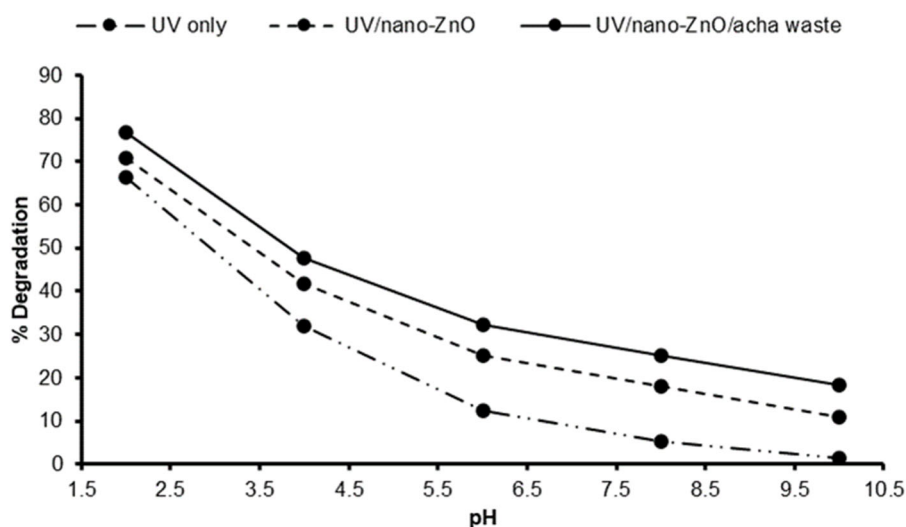


Fig 6. Effect of pH on the degradation of metronidazole using UV, UV/nano-ZnO and UV/nano-ZnO/acha waste systems

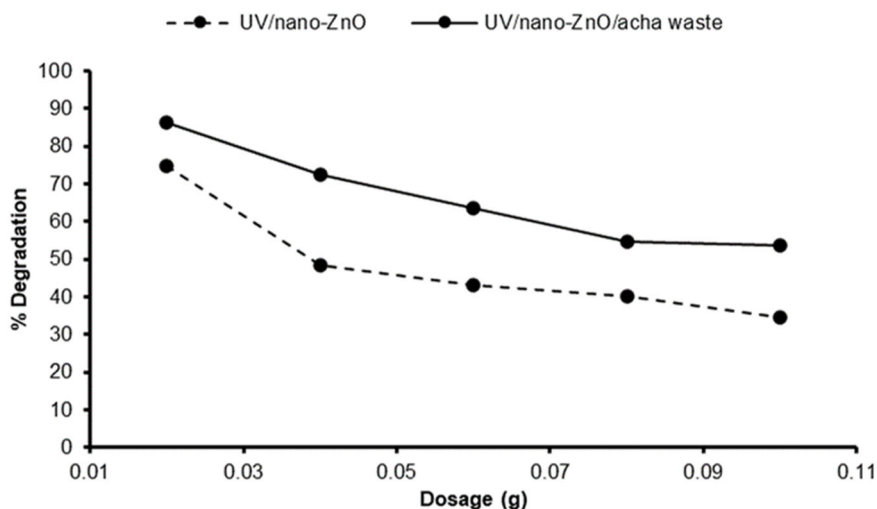


Fig 7. Effect of catalyst dosages on the degradation of metronidazole using UV/nano-ZnO and UV/nano-ZnO/acha waste systems

have resulted from increased blockage of the incident UV light with increasing catalyst dosages. Sheikhsamany et al. [31] and Farzadkia et al. [15] observed similar results.

Kinetics of Degradation

Applying the data of the effect of time of exposure, the degradation of MNZ solution by UV light only, UV/nano-ZnO, and UV/nano-ZnO/acha waste treatment systems follow the pseudo-first-order kinetics with respect to the concentration of MNZ in the solution (Eq. (2)). The integration of Eq. (2) gives Eq. (3).

$$r = \frac{d\text{MNZ}}{d_t} = k\text{MNZ} \quad (2)$$

$$\ln\left(\frac{\text{MNZ}_0}{\text{MNZ}_t}\right) = kt \quad (3)$$

where, MNZ_0 is the initial MNZ concentration of the solution in mg/L and MNZ_t is the concentration of MNZ at time t , the rate constant (k) was obtained from the slope of the plot of $\ln \text{MNZ}_0/\text{MNZ}_t$ versus time (t).

According to Fig. 8, the rate constant (k) and the R^2 values for MNZ degradation are presented in Table 3. The high R^2 values obtained for the three treatment methods are an indication that the degradation of MNZ conforms to the pseudo-first-order kinetic model. The rate constants showed that the UV treatment system is not

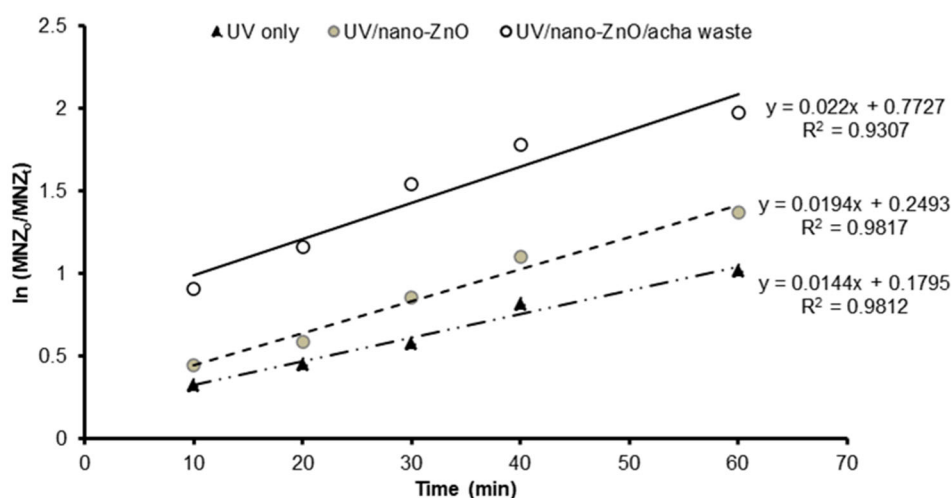


Fig 8. The kinetic plot of the degradation of metronidazole in UV, UV/nano-ZnO and UV/nano-ZnO/acha waste systems

Table 3. Metronidazole degradation kinetic constants

Treatment technique	Kinetic constant (min ⁻¹)	R ²
UV only	0.0144	0.9812
UV/nano-ZnO	0.0194	0.9817
UV/nano-ZnO/acha waste system	0.0220	0.9307

Table 4. Comparison of the photocatalytic degradation of metronidazole

Photocatalytic methods	Efficiency (%)	References
UV/TiO ₂	99.5	[15]
UV/TiO ₂	86.1	[32]
UV/ZnO	60.3	[32]
UV/Fe ₃ O ₄ /TiO ₂ /biochar	80.0	[29]
UV/nanoCoFe ₂ O ₄ @methycellulose	85.3	[33]
UV/ Ag-ZnO/graphite	88.5	[34]
Solar/ Ag-ZnO/graphite	97.3	[34]
UV/TiO ₂ -P25 + PbS	95.0	[35]
UV	64.0	[35]
UV/nano-ZnO	74.7	Present study
UV/nano-ZnO/acha waste	86.1	Present study

as effective as the treatment systems involving the catalysts. The UV treatment catalyzed with zinc oxide nanoparticles is 1.3 times faster in comparison to UV only, whereas the use of nano-ZnO/acha waste is 1.5 times faster. The fast reaction rate with nano-ZnO/acha waste highlights its excellent removal of the MNZ from aqueous solution, owing to a synergistic influence of UV, zinc oxide nanoparticles and acha waste. The removal efficiency of MNZ in the present study compared with other photocatalytic treatment methods is presented in Table 4. The table indicated that the photocatalytic degradation of MNZ by zinc oxide nanoparticles supported on acha waste shows satisfactory performance.

■ CONCLUSION

This study employs the use of UV light, a promising technique in the field of AOPs, to degrade MNZ using zinc oxide nanoparticles and nano-ZnO/acha waste composite as photocatalysts. The percentage degradation of MNZ obtained using UV light combined with nano-ZnO is approximately 2 times faster when compared to the use of UV light only, whereas, the introduction of the nano-ZnO/acha waste composite also enhanced the photocatalytic ability, thereby allowing more degradation of MNZ wastewater to occur. Generally, experimental results have

proven that the UV/nano-ZnO and UV/nano-ZnO/acha waste treatment systems had better performance for the degradation of MNZ wastewater than UV alone.

■ AUTHOR CONTRIBUTIONS

Olushola Sunday Ayanda conceived and designed the experiments. Blessing Oluwatobi Adeleye and Omolola Helen Aremu performed the experiment. Folasade Busayo Ojobola, Michael John Klink and Simphiwe Maurice Nelana contributed to the characterization of the materials. Olusola Solomon Amodu and Oyedele Oyebamiji Oketayo analyzed and interpreted the data, Olushola Sunday Ayanda wrote the paper, and Olayide Samuel Lawal revised the manuscript. All authors agreed to the final version of this manuscript.

■ REFERENCES

- [1] Kapoor, D., 2015, Impact of pharmaceutical industries on environment, health and safety, *J. Crit. Rev.*, 2 (4), 25–30.
- [2] Manasa, R.L., and Mehta, A., 2020, “Wastewater: Sources of Pollutants and Its Remediation” in *Environmental Biotechnology*, Vol. 2, Eds. Gothandam, K.M., Ranjan, S., Dasgupta, N., and Lichtfouse, E., Springer, Cham, 197–219.

- [3] Chen, J.Q., Shang, C., and Cai, X.L., 2013, Application of cyclonic floatation integrated technology in low oil content sewage treatment, *China Pet. Mach.*, 41 (9), 62–66.
- [4] Hemphill, A., Müller, N., and Müller, J., 2019, Comparative pathobiology of the intestinal protozoan parasites *Giardia lamblia*, *Entamoeba histolytica*, and *Cryptosporidium parvum*, *Pathogens*, 8 (3), 116.
- [5] Ceruelos, A.H., Romero-Quezada, L.C., Ruvalcaba Ledezma, J.C., and López Contreras, L., 2019, Therapeutic uses of metronidazole and its side effects: An update, *Eur. Rev. Med. Pharmacol. Sci.*, 23 (1), 397–401.
- [6] Kannigadu, C., and N'Da, D.D., 2020, Recent advances in the synthesis and development of nitroaromatics as anti-infective drugs, *Curr. Pharm. Des.*, 26 (36), 4658–4674.
- [7] Edwards, D.I., 1993, Nitroimidazole drugs-action and resistance mechanisms I. Mechanism of action, *J. Antimicrob. Chemother.*, 31 (1), 9–20.
- [8] Nunn, A.J., 2021, “Routes of Administration and Formulations” in *Paediatric Clinical Pharmacology*, Eds. Jacqz-Aigrain, E., and Choonara, I., CRC Press, Boca Raton, Florida, 219–233.
- [9] Arslan-Alaton, I., and Dogruel, S., 2004, Pre-treatment of penicillin formulation effluent by advanced oxidation processes, *J. Hazard. Mater.*, 112 (1-2), 105–113.
- [10] Rozas, O., Contreras, D., Mondaca, M.A., Pérez-Moya, M., and Mansilla, H.D., 2010, Experimental design of Fenton and photo-Fenton reactions for the treatment of ampicillin solutions, *J. Hazard. Mater.*, 177 (1-3), 1025–1030.
- [11] Ayanda, O.S., Nelana, S.M., Petrik, L.F., and Naidoo, E.B., 2018, Kinetic study of ultrasound degradation of 2,2-bis(4-hydroxyphenyl)propane assisted by nFe/TiO₂ composite, *J. Adv. Oxid. Technol.*, 21 (1), 170–177.
- [12] Deng, Y., and Zhao, R., 2015, Advanced oxidation processes (AOPs) in wastewater treatment, *Curr. Pollut. Rep.*, 1 (3), 167–176.
- [13] Farzadkia, M., Esrafil, A., Baghapour, M.A., Shahamat, Y.D., and Okhovat, N., 2014, Degradation of metronidazole in aqueous solution by nano-ZnO/UV photocatalytic process, *Desalin. Water Treat.*, 52 (25-27), 4947–4952.
- [14] Fang, Z., Chen, J., Qiu, X., Qiu, X., Cheng, W., and Zhu, L., 2011, Effective removal of antibiotic metronidazole from water by nanoscale zero-valent iron particles, *Desalination*, 268 (1-3), 60–67.
- [15] Farzadkia, M., Bazrafshan, E., Esrafil, A., Yang, J.K., and Shirzad-Siboni, M., 2015, Photocatalytic degradation of metronidazole with illuminated TiO₂ nanoparticles, *J. Environ. Health Sci. Eng.*, 13 (1), 35.
- [16] Garí, J.A., 2002, “Review of the African Millet Diversity” in *International Workshop on Fonio, Food Security and Livelihood Among the Rural Poor in West Africa*, November 19-22, 2001, Bamako, Mali.
- [17] Cruz, J.F., Béavogui, F., and Dramé, D., 2011, *Le Fonio, Une Céréale Africaine*, Agricultures tropicales en poche, Quae Editions, Presses Agronomiques de Gembloux, Belgium.
- [18] Ayanda, O.S., Aremu, O.H., Akintayo, C.O., Sodeinde, K.O., Igboama, W.N., Oseghe, E.O., and Nelana, S.M., 2011, Sonocatalytic degradation of amoxicillin from aquaculture effluent by zinc oxide nanoparticles, *Environ. Nanotechnol. Monit. Manage.*, 16, 100513.
- [19] Awe, A.A., Opeolu, B.O., Fatoki, O.S., Ayanda, O.S., Jackson, V.A., and Snyman, R., 2020, Preparation and characterisation of activated carbon from *Vitis vinifera* leaf litter and its adsorption performance for aqueous phenanthrene, *Appl. Biol. Chem.*, 63 (1), 12.
- [20] Alimi, B.A., Workneh, T.S., and Femi, F.A., 2021, Fabrication and characterization of edible films from acha (*Digitalia exilis*) and iburu (*Digitalia iburua*) starches, *CyTA-J. Food*, 19 (1), 493–500.
- [21] Alibeigi, A.N., Javid, N., Amiri Gharaghani, M., Honarmandrad, Z., and Parsaie, F., 2021, Synthesis, characteristics, and photocatalytic activity of zinc oxide nanoparticles stabilized on the stone surface for degradation of metronidazole from aqueous

- solution, *Environ. Health Eng. Manage. J.*, 8 (1), 55–63.
- [22] Jan, H., Shah, M., Usman, H., Khan, A., Zia, M., Hano, C., and Abbasi, B.H., 2020, Biogenic synthesis and characterization of antimicrobial and anti-parasitic zinc oxide (ZnO) nanoparticles using aqueous extracts of the Himalayan columbine (*Aquilegia pubiflora*), *Front. Mater.*, 7, 00249.
- [23] Wei, C., Ge, Y., Liu, D., Zhao, S., Wei, M., Jiliu, J., Hu, X., Quan, Z., Wu, Y., Su, Y., Wang, Y., and Cao, L., 2022, Effects of high-temperature, high-pressure, and ultrasonic treatment on the physicochemical properties and structure of soluble dietary fibers of millet bran, *Front. Nutr.*, 8, 820715.
- [24] Bello, O.M., Ogbesejana, A.B., Balkisu, A., Osibemhe, M., Musa, B., and Oguntoye, S.O., 2022, Polyphenolic fractions from three millet types (Fonio, Finger millet, and Pearl millet): Their characterization and biological importance, *Clin. Complementary Med. Pharmacol.*, 2 (1), 100020.
- [25] Al-Kordy, H.M.H., Sabry, S.A., and Mabrouk, M.E.M., 2021, Statistical optimization of experimental parameters for extracellular synthesis of zinc oxide nanoparticles by a novel haloaliphilic *Alkalibacillus* sp. W7, *Sci. Rep.*, 11 (1), 10924.
- [26] Mohan, A.C., and Renjanadevi, B., 2016, Preparation of zinc oxide nanoparticles and its characterization using scanning electron microscopy (SEM) and X-ray diffraction (XRD), *Procedia Technol.*, 24, 761–766.
- [27] Moradmand Jalali, H., and Dezhampannah, H., 2021, Kinetic investigation of photo-degradation of amoxicillin, ampicillin, and cloxacillin by semiconductors using Monte Carlo simulation, *Chem. Eng. Commun.*, 208 (2), 159–165.
- [28] Khezrianjoo, S., and Revanasiddappa, H.D., 2013, Photocatalytic degradation of acid yellow 36 using zinc oxide photocatalyst in aqueous media, *J. Catal.*, 2013, 582058.
- [29] Isai, K.A., and Shrivastava, V.S., 2019, Photocatalytic degradation of methylene blue using ZnO and 2% Fe–ZnO semiconductor nanomaterials synthesized by sol–gel method: A comparative study, *SN Appl. Sci.*, 1 (10), 1247.
- [30] Asgharzadeh, F., Gholami, M., Jafari, A.J., Kermani, M., Asgharnia, H., and Kalantary, R.R., 2019, Heterogeneous photocatalytic degradation of metronidazole from aqueous solutions using Fe₃O₄/TiO₂ supported on biochar, *Desalin. Water Treat.*, 175, 304–315.
- [31] Sheikhsamany, R., Faghihian, H., and Fazaeli, R., 2022, Synthesis of novel HKUST-1-based SnO₂ porous nanocomposite with the photocatalytic capability for degradation of metronidazole, *Mater. Sci. Semicond. Process.*, 138, 106310.
- [32] Tran, M.L., Fu, C.C., and Juang, R.S., 2018, Removal of metronidazole by TiO₂ and ZnO photocatalysis: A comprehensive comparison of process optimization and transformation products, *Environ. Sci. Pollut. Res.*, 25 (28), 28285–28295.
- [33] Nasiri, A., Tamaddon, F., Mosslemin, M.H., Gharaghani, M.A., and Asadipour, A., 2019, New magnetic nanobiocomposite CoFe₂O₄@methylcellulose: Facile synthesis, characterization, and photocatalytic degradation of metronidazole, *J. Mater. Sci.: Mater. Electron.*, 30 (9), 8595–8610.
- [34] Tran, M.L., Nguyen, C.H., Fu, C.C., and Juang, R.S., 2019, Hybridizing Ag-Doped ZnO nanoparticles with graphite as potential photocatalysts for enhanced removal of metronidazole antibiotic from water, *J. Environ. Manage.*, 252, 109611.
- [35] Stando, K., Kasprzyk, P., Felis, E., and Bajkacz, S., 2021, Heterogeneous photocatalysis of metronidazole in aquatic samples, *Molecules*, 26 (24), 7612.
- [36] Taoufik, N., Boumya, W., Achak, M., Sillanpää, M., and Barka, N., 2021, Comparative overview of advanced oxidation processes and biological approaches for the removal pharmaceuticals, *J. Environ. Manage.*, 288, 112404.